

Supporting Information

Wagner et al. 10.1073/pnas.1008053107

SI Materials and Methods

Materials. Chemicals were from Sigma-Aldrich unless otherwise stated. SERVA Blue G was from Serva. n-dodecyl- β -D-malto-pyranoside (DDM) and n-dodecyl-N,N-dimethylamine-N-oxide (LDAO) were from Anatrace. Anti-FLAG M2 affinity gel and 3 \times FLAG peptide were from Sigma. GelBond PAG Film was from Lonza. Protease inhibitor mixture complete EDTA-free was from Roche. DyLight conjugated antibodies (680 nm and 800 nm, respectively) were from Pierce. Antibase antibody recognizing PrgH and PrgK was previously described (1).

Bacterial Strains, Plasmids, and Culture Conditions. Bacterial strains and plasmids used in this study are listed in Table S2. The low copy number rhamnose expression plasmid pSB3398 was constructed as follows. The rhamnose promoter P^{rhaBAD} and the regulatory genes $rhaR$ and $rhaS$ were amplified from pTACO2 (2) and cloned into pBAD24 (3), replacing $araC$ and the P^{araBAD} promoter and resulting in pRha24. The kanamycine resistance marker $aphA1$ was amplified from pGFPe (4) and cloned into pWSK-30 (5), replacing bla . Finally, a fragment harboring $rhaR$, $rhaS$, P^{rhaBAD} , and the multiple cloning site and transcriptional terminator rmB was amplified from pRha24 and combined with an amplified fragment harboring the pSC101 origin of replication and $aphA1$. Cultures of *S. Typhimurium* were grown in Luria broth (LB) supplemented with 0.3 M NaCl and antibiotics as necessary. Cultures were grown with low aeration to enhance expression of genes of pathogenicity island 1 (SPI-1).

Cell Fractionation. Cell fractionation was carried out as described before (6) with some modifications. Crude membranes were precipitated at 235,000 $\times g$ for 1 h, resuspended in buffer M, and loaded on top of a 29–50% (wt/wt) continuous sucrose gradient, which was made using a Gradient Station (Biocomp). Inner and outer membranes were separated by centrifugation at 285,000 $\times g$ for 13 h; 12 fractions of \sim 1.1 mL were collected using the Gradient Station. Inner membranes were enriched in fractions 6 and 7, and outer membranes were enriched in fractions 9 and 10 (Fig. S1).

Blue Native-PAGE. Blue native-PAGE (BN-PAGE) was carried out as described previously (7). 2D BN-PAGE was performed as described (8) using a 3–12% gradient gel in the first dimension and a 12% glycine SDS/PAGE or 10% Tricine SDS/PAGE, respectively, in the second dimension. The NativePAGE Novex Bis-Tris Gel System (Invitrogen) was used when Western blotting was performed. For BN-PAGE of whole-cell lysates, 0.4 OD₆₀₀ units of cells were resuspended in 10 μ L buffer KCl (2 mg/mL lysozyme, complete EDTA-free, 50 mM triethanolamine, pH 7.5, 250 mM sucrose, 1 mM EDTA) and incubated for 30 min on ice; 70 μ L BN resuspension buffer (750 mM aminocaproic acid, 50 mM Bis-Tris, pH 7.0) were added, and cells were lysed by three cycles of freeze-thawing. DDM was added to a final concentration of 1%, and the cell lysates were mixed at 4 $^{\circ}$ C for 1 h. The lysates were cleared of debris and unsolubilized material by centrifugation at 20,000 $\times g$ for 15 min at 4 $^{\circ}$ C; 45 μ L supernatant were transferred to fresh tubes containing 5 μ L 10 \times BN loading dye [5% (wt/vol) SERVA Blue G, 500 mM aminocaproic acid] and mixed. Subsequently, 25 μ L per well were run on a NativePAGE Novex Bis-Tris Gel System.

Identification of Type III Secretion System Components by MS. Stained protein bands/spots were excised from polyacrylamide gels, washed, digested with modified trypsin, and extracted manually as described (9).

Liquid chromatography tandem MS on the Waters/Micromass Q-ToF Ultima. In gel, tryptic digested protein mixture was analyzed by liquid chromatography tandem MS (LC MS/MS) on a Waters CapLC coupled in line with a Waters/Micromass Q-ToF Ultima mass spectrometer. The instrument is calibrated, and MS/MS conditions are optimized with direct infusion of a Glu-fibrinogen [$m/z = 785.85$ (2+)] calibrant at a final concentration of \sim 200 fmol/ μ L. After in gel trypsin digestion, 5 μ L of the sample are injected onto a 100- μ m inner diameter \times 15 cm Atlantis C18 column (Waters) for LC MS/MS analysis. A 95-min gradient (initial HPLC conditions were 95% Buffer A and 5% Buffer B with the following linear gradient: 3 min, 5% B; 43 min, 37% B; 75 min, 75% B; and 85 min, 95% B) with a flow rate of 500 nL/min is used to obtain good peptide separation. Buffer A consists of 98% water, 2% acetonitrile, 0.1% acetic acid, and 0.01% TFA. Buffer B contains 80% acetonitrile, 20% water, 0.09% acetic acid, and 0.01% TFA. Data-dependent acquisition is enabled so that when the total ion current increased above the 1.5 counts/s threshold, the mass spectrometer switches automatically from MS to MS/MS modes. To ensure optimal fragmentation of selected precursor peaks, a collision energy ramp was set for the different mass sizes and charge states, giving preference to double- and triple-charged species for fragmentation.

LC-MS/MS on the linear ion trap Orbitrap. The linear ion trap (LTQ) Orbitrap is equipped with a Waters nanoAcquity ultra performance liquid chromatography system and uses a Waters Symmetry C18 180 μ m \times 20 mm trap column and a 1.7- μ m 75 μ m \times 250 mm nanoAcquity UPLC column (35 $^{\circ}$ C) for peptide separation. The flow rate is 300 nL/min with Buffer A (100% water, 0.1% formic acid) and Buffer B (100% CH₃CN, 0.075% formic acid). A linear gradient (51 min) is run with 5% buffer B at initial conditions, 50% B at 50 min, and 85% B at 51 min. MS (m/z range = 400–2,000 at average resolving power of 60,000) is acquired in the Orbitrap using one microscan and in parallel with six data-dependant MS/MS acquisitions (based on the top six most intense MS peaks) in the LTQ. Peaks targeted for MS/MS fragmentation by collision induced dissociation (CID) were first isolated with a 2-Da window followed by a normalized collision energy of 35%. Dynamic exclusion was activated where former target ions were excluded for 30 s. Each MS Orbitrap scan took 1.4 s to acquire, whereas up to six MS/MS scans were acquired over an average time of 1 s; the total cycle time for both MS and MS/MS acquisition was 2.4 s.

Database search. All raw LC-MS/MS spectral data were searched in-house using the Mascot algorithm (Matrix Science) with the Mascot Distiller program used to generate Mascot compatible files. The Mascot Distiller program combines and centroids sequential MS/MS scans from profile data that have the same precursor ion. Charge state for +5 or less was preferentially located with a signal to noise ratio of 1.2 or greater, and a peak list was generated for database searching. The parameters used in the database search were (i) searched against the *Salmonella* database (UniprotSMTyphi_2009), (ii) four miscleavages setting was used for trypsin digestion, (iii) error tolerances were set based on the instrument that was used (i.e., 25 ppm for MS and 0.6 Da for MS/MS on LTQ-Orbitrap), (iv) variable settings were used for oxidation of methionines and propanimide modification (gel), and carboamidomethylation of cysteines, and (v) preferential charge state of \leq 5+ was used. Using the Mascot database search algorithm, a protein was considered identified when Mascot listed it as a significant match/score ($P < 0.05$) with the proper enzymatic cleavage sites. The Mascot significance score match is based on a MOWSE score and relies on multiple matches to more than one

peptide from the same protein. Additional constraints were also imposed for protein identifications: matched protein (based on accession number) must have two or more matching peptides and MS/MS fragmentation must show at least three consensus amino acid sequence.

Immunoprecipitation of Export Apparatus Components. FLAG-tagged export apparatus components were immunoprecipitated from purified inner membranes using the ANTI-FLAG M2 affinity gel according to the recommendations of the manufacturer. For BN-PAGE analysis, precipitated complexes were eluted with 150 ng/ μ L 3 \times FLAG peptide in BN resuspension buffer supplemented with 0.5% DDM and subsequently analyzed by 1D or 2D BN-PAGE. Proteins in 1D BN gels were visualized using colloidal Coomassie stain (10). Proteins in 2D BN gels were visualized using an MS-compatible silver stain (11). For negative-stain electron microscopy, precipitated complexes were eluted with 150 ng/ μ L 3 \times FLAG peptide in PBS supplemented with 0.5% DDM and subsequently analyzed by transmission electron microscopy.

Levels of Export Apparatus Components. The levels of FLAG-tagged export apparatus components in purified inner membranes were assessed by Western blotting. Export apparatus components were visualized using mouse anti-FLAG (M2) primary antibodies and anti-mouse infrared fluorescent (emission 800 nm) secondary antibodies. Bands were quantified using the Odyssey imaging system (Li-Cor). PrgH was used as a loading control. PrgH was visualized using rabbit antineedle complex (NC) primary antibodies and anti-rabbit infrared fluorescent (emission 680 nm) secondary antibodies.

Coordinated Expression of Type III Secretion System Components. The experimental setup to assess whether export apparatus components were able to induce de novo assembly of bases involved a set of strains of *S. Typhimurium* (SB1892 and SB2091) in which expression of HilA, which itself controls expression of the base components, was put under control of an arabinose-inducible promoter. In these strains, either *invA* (SB1892) or *spaPQRS* (SB2091) were deleted from the chromosome. FLAG-tagged alleles of respective proteins (*invA*^{FLAG} or *spaP*^{FLAG}*QRS*) were present in a low copy number plasmid (pSB3405 and pSB3704, respectively), and their expression was under the control of a rhamnose-inducible promoter. Base expression was induced by the addition of 0.02% arabinose. The inducer was washed away, and expression of the base components was blocked by the addition of the repressor fucose (5 mM). Sixty minutes later, expression of export apparatus components (either *InvA*^{FLAG} or *SpaP*^{FLAG}*QRS*) was induced by the addition of rhamnose (100 μ M). Samples were harvested 30 and 60 min thereafter, and proteins of whole-cell lysates were separated by BN-PAGE or SDS/PAGE and analyzed by Western blotting. NC/bases, PrgH monomers (in BN-PAGE gels), PrgH, and PrgK were visualized using rabbit anti-NC antibodies primary and anti-rabbit infrared fluorescent (emission 680 nm, except for PrgH monomers in which an antibody emitting at 800 nm was used) secondary antibodies. FLAG-tagged export apparatus components were visualized using mouse anti-FLAG (M2) primary antibodies and anti-mouse infrared fluorescent (emission 800 nm) secondary antibodies. Protein bands were quantified using the Odyssey imaging system (Li-Cor). Because the assembly of the needle filament resulted in a shift in native mass of the complex, it was possible to distinguish between bases and NCs. The levels of bases/NC were quantified using two rectangular fields in the 680-nm channel. The size of the lower (base) field was chosen so that it would cover the base before expression of export apparatus components, hence before assembly of the needle filament. The size of the upper (NC) field was chosen so that it would cover the fluorescence signal of the export apparatus component in the 800-nm channel.

To ensure that only a stable pool of NC components was being observed, we assessed their turnover in this experimental setup. To this end, expression of NC components was induced by the addition of 0.02% arabinose, and after 5 h, the inducer was washed away and further expression was blocked by the addition of 5 mM fucose. Samples were taken at time points 0, 30, 60, 90, and 120 min thereafter. Protein synthesis was blocked in a parallel set of samples by the addition of chloramphenicol, and samples were taken at the corresponding time points. Proteins of whole-cell lysates of *S. Typhimurium* harvested at the indicated time points were separated by SDS/PAGE and analyzed by Western blotting. Proteins were visualized as described above. Comparison of the levels of NC components after blockage of protein synthesis vs. the levels after repression of their expression by addition of fucose indicated that no significant turnover of NC components occurs under these experimental conditions (Fig. S7). Furthermore, to test the ability of fucose-treated cells to carry out protein synthesis at this late phase of growth, expression of *SpaPQRS* was induced by the addition of 100 μ M rhamnose after 90 min (lane 11).

To assess if base assembly is initiated after deployment of the export apparatus, a similar setup was used as describe above. The setup to assess if export apparatus components were able to efficiently associate with preassembled bases involved a set of strains (SB2156 and SB2157) in which expression of HilA, which itself controls the expression of the base components, was placed under the control of an arabinose-inducible promoter. The expression of FLAG-tagged alleles of the export apparatus components *InvA* or *SpaPQRS* was under the control of a rhamnose-inducible promoter. The *P*^{tha} *invA*^{FLAG}/*spaP*^{FLAG}*QRS* alleles, respectively, were introduced into the chromosome by allelic exchange with the *malE* and *malK* promoter region. Regulated expression of NC components was fine-tuned such that the ratio of *InvA*^{FLAG}/*SpaP*^{FLAG} to PrgH, respectively, was comparable with the ratio in a wild-type strain (Fig. 5B Lower). In these strains, base expression was induced by the addition of 0.02% arabinose. The inducer was washed away, and expression of the base components was blocked by the addition of the repressor fucose (5 mM). Sixty minutes later, expression of export apparatus components (either *InvA*^{FLAG} or *SpaP*^{FLAG}*QRS*) was induced by the addition of rhamnose (1 mM for *SpaP*^{FLAG}*QRS* and 2 mM for *InvA*^{FLAG}). Samples were harvested 30 min thereafter, and proteins of whole-cell lysates were separated by BN-PAGE or SDS/PAGE and analyzed by Western blotting as described above. The relative association of *SpaP* and *InvA* with the NC was determined by calculating the ratio of the fluorescence signals *SpaP*/NC and *InvA*/NC, respectively. Because expression of *SpaPQRS* induced the formation of bases from preexisting protomers (Fig. 4), it was important to distinguish between the association of *SpaP*/*InvA* with truly preexisting bases and with de novo assembled bases from preexisting protomers. Because expression of *InvA* did not induce the de novo assembly of bases from preexisting protomers, there is no incorporation into those bases, and hence, *InvA* is only incorporated into preexisting bases. To the contrary, the experiment shown in Fig. 4 showed that *SpaP* did predominantly incorporate into de novo assembled bases from preexisting protomers, and hence, there is very limited incorporation of *SpaP* into preexisting bases.

The setup to assess if export apparatus components were able to efficiently associate with de novo synthesized bases involved a set of strains (SB2093 and SB2092) in which expression of HilA, which itself controls the expression of the base components, was placed under the control of an arabinose-inducible promoter. In these strains, either an *invA*^{FLAG} or a *spaP*^{FLAG} allele was introduced into the chromosome by allelic exchange, and *prgHIJK* was deleted from the chromosome. The genes encoding the based components (*prgHIJK* and *invGH*) were present in a low copy number plasmid (pSB3418), and their expression was under the control of a rhamnose-inducible promoter. Regulated ex-

pression of NC components was fine-tuned such that the ratio of InvA^{FLAG}/SpaP^{FLAG} to PrgH, respectively, was comparable with the ratio in a wild-type strain. In these strains, expression of the export apparatus components was induced by the addition of 0.02% arabinose. The inducer was washed away, and expression of export apparatus components was blocked by the addition of the repressor fucose (5 mM). Sixty minutes later, expression of base components was induced by the addition of rhamnose (250 μ M). Samples were harvested 30 min thereafter, and proteins of whole-cell lysates were separated by BN-PAGE or SDS/PAGE and analyzed by Western blotting as described above. The relative association of SpaP and InvA with the NC was determined by calculating the ratio of the fluorescence signals SpaP/NC and InvA/NC, respectively.

Stability of Type III Secretion System Bases. The stability of NC/bases was assessed by using a protocol for BN-PAGE/Western blotting, which is slightly modified from the one described above. Protein complexes of purified inner membrane fractions were solubilized in BN resuspension buffer supplemented with 0.5% DDM and increasing amounts of SDS (0.1–0.5%). Samples were incubated at 20 °C for 1 h, BN loading dye was added, and samples were run on a NativePAGE Novex Bis-Tris Gel System followed by Western blotting. NC/bases were visualized using rabbit anti-NC primary antibodies and anti-rabbit infrared fluorescent (emission 800 nm) secondary antibodies. Bands corresponding to NC/bases were quantified using the Odyssey imaging system (Li-Cor).

NC Expression, Purification, and PAGE Analysis. Seed cultures were grown overnight at 37 °C in LB supplemented with 0.3 M NaCl and appropriate antibiotics. Cultures were diluted 1:10 in the same medium and grown to an OD of 0.5 before inducing expression of hila by adding arabinose to a concentration of 0.012%. During purification, samples were kept at 4 °C unless stated otherwise. Bacteria were harvested at early stationary phase, resuspended in 150 mM sodium phosphate (pH 7.4), 0.5 M sucrose, 1.4 mg/mL hen egg lysozyme, and 12.2 mM EDTA, and incubated on ice while stirring for 45 min followed by 15 min at 37 °C. Cells were lysed with 0.35% LDAO before adding 500 mM NaCl and 20 mM MgCl₂ to the lysate. Cell debris was removed by low-speed centrifugation at 29,600 \times g for 20 min, and NCs were pelleted by high-speed centrifugation at 177,500 \times g for 150 min. The pellet was resuspended in a 0.5% LDAO, 10 mM sodium phosphate (pH 7.4), 0.5 M NaCl, and 5 mM EDTA buffer, and adjusted to a final concentration of 27.5% wt/vol of CsCl. Samples were centrifuged for 16 h at 339,000 \times g; 0.5-mL aliquots were combined with 2.4 mL CsCl-free buffer and pelleted at 438,000 \times g for 30 min. The needle complexes were resuspended in 0.1 mL 0.1% LDAO, 10 mM sodium phosphate (pH 7.4), and 0.5 M NaCl. The composition of NC preparations of strains harboring FLAG-tagged alleles of InvA and SpaP, respectively, was assessed by SDS/PAGE and BN-PAGE, respectively, followed by Western blotting. For

BN-PAGE, purified NCs were diluted in 18 μ L PBS/350 mM NaCl/5 mM EDTA/0.1% LDAO; 2 μ L 10 \times BN loading dye was added. Samples were mixed and subsequently run on a Native-PAGE Novex Bis-Tris Gel System followed by Western blotting. NCs/bases were visualized using rabbit anti-NC antibodies primary and anti-rabbit infrared fluorescent (emission 680 nm) secondary antibodies. FLAG-tagged export apparatus components were visualized using mouse anti-FLAG (M2) primary antibodies and anti-mouse infrared fluorescent (emission 800 nm) secondary antibodies. Bands corresponding to NCs/bases and FLAG-tagged export apparatus components were quantified using the Odyssey imaging system (Li-Cor).

Electron Microscopy and Image Processing. NCs purified by anti-FLAG immunoprecipitation were applied to glow-discharged carbon-coated 200-mesh hexagonal Cu-grids. For negative stain images, 5 μ L of sample were applied to the grid and subsequently stained with 2% phosphotungstic acid, pH 7.0. Images were acquired at 135,000-fold magnification in a Tecnai Bitwin TEM (FEI Company) at 80 kV using the Morada Soft Imaging system and a 6M pixel CCD camera (Olympus). NCs purified by the previously described stringent protocol (12) were applied to glow-discharged carbon-coated 400-mesh hexagonal Cu/Pd-grids. For negative stain images, 5 μ L of sample were applied to the grid and subsequently stained with 2% PTA, pH 7.0. Overview images were acquired at 56,000-fold magnification in a Morgagni TEM (FEI Company) at 80kV using an 11-megapixel CCD camera. For cryo-electron microscopy, 5 μ L of sample were applied to glow-discharged grids before vitrification by plunge-freezing in liquid ethane. Low-dose data were collected with a FEI Tecnai Polara at 300 kV using a Gatan Ultrascan 4000 UHS CCD camera (16 megapixel, 4 \times 4 k, 15 μ m pixel size). Images were acquired at 71,949-fold magnification (2.08 \AA /pixel) with under focus values ranging from 1.2 to 3.5 μ m. The contrast reversals imposed by the contrast transfer function of the objective lens were corrected for each image using the defocus values determined by the program CTFFIND3 (13). Subsequent image data processing was done using IMAGIC-5 (Image Science Software GmbH) and XMIPP (14). Individual particle projections were extracted, combined in one dataset (256 \times 256 pixelbox), and subjected to classification by several rounds of multivariate statistical analysis (MSA) and maximum likelihood analysis. Class averages were used in a cross-correlation-based multireference alignment (MRA) procedure to obtain Euler angles for 3D reconstruction. 3D maps were generated without enforcing symmetry (C1), because the actual symmetry of the *Salmonella* needle complex has not been unambiguously determined and maps were filtered to 22 \AA of resolution. Surface-rendering images were obtained by using the software package CHIMERA (15).

1. Sukhan A, Kubori T, Wilson J, Galán JE (2001) Genetic analysis of assembly of the *Salmonella enterica* serovar Typhimurium type III secretion-associated needle complex. *J Bacteriol* 183:1159–1167.
2. Wagner S, et al. (2008) Tuning *Escherichia coli* for membrane protein overexpression. *Proc Natl Acad Sci USA* 105:14371–14376.
3. Guzman LM, Belin D, Carson MJ, Beckwith J (1995) Tight regulation, modulation, and high-level expression by vectors containing the arabinose PBAD promoter. *J Bacteriol* 177:4121–4130.
4. Drew D, et al. (2005) A scalable, GFP-based pipeline for membrane protein overexpression screening and purification. *Protein Sci* 14:2011–2017.
5. Wang RF, Kushner SR (1991) Construction of versatile low-copy-number vectors for cloning, sequencing and gene expression in *Escherichia coli*. *Gene* 100:195–199.
6. Wagner S, et al. (2007) Consequences of membrane protein overexpression in *Escherichia coli*. *Mol Cell Proteomics* 6:1527–1550.
7. Schagger H, von Jagow G (1991) Blue native electrophoresis for isolation of membrane protein complexes in enzymatically active form. *Anal Biochem* 199:223–231.
8. Klepsch M, et al. (2008) Immobilization of the first dimension in 2D blue native/SDS-PAGE allows the relative quantification of membrane proteomes. *Methods* 46:48–53.
9. Peltier JB, et al. (2002) Central functions of the luminal and peripheral thylakoid proteome of *Arabidopsis* determined by experimentation and genome-wide prediction. *Plant Cell* 14:211–236.
10. Neuhoff V, Arold N, Taube D, Ehrhardt W (1988) Improved staining of proteins in polyacrylamide gels including isoelectric focusing gels with clear background at nanogram sensitivity using Coomassie Brilliant Blue G-250 and R-250. *Electrophoresis* 9:255–262.
11. Shevchenko A, Wilm M, Vorm O, Mann M (1996) Mass spectrometric sequencing of proteins silver-stained polyacrylamide gels. *Anal Chem* 68:850–858.
12. Marlovits TC, et al. (2004) Structural insights into the assembly of the type III secretion needle complex. *Science* 306:1040–1042.
13. Mindell JA, Grigorieff N (2003) Accurate determination of local defocus and specimen tilt in electron microscopy. *J Struct Biol* 142:334–347.
14. Scheres SH, Valle M, Grob P, Nogales E, Carazo JM (2009) Maximum likelihood refinement of electron microscopy data with normalization errors. *J Struct Biol* 166: 234–240.
15. Pettersen EF, et al. (2004) UCSF Chimera—a visualization system for exploratory research and analysis. *J Comput Chem* 25:1605–1612.

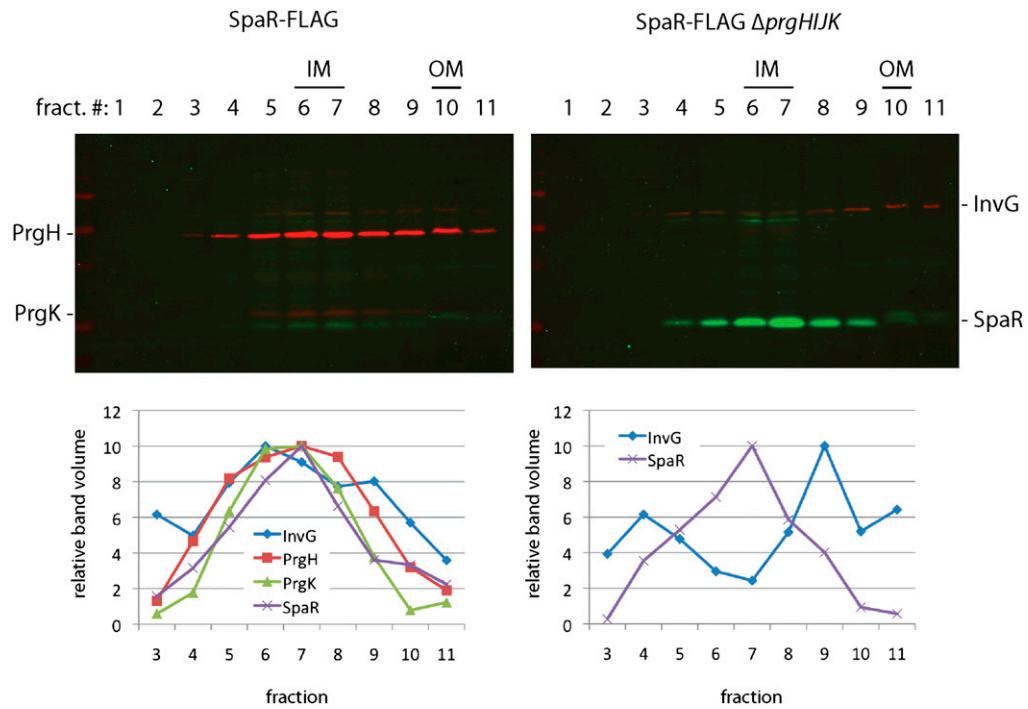


Fig. S1. The type III secretion system (T3SS) needle complex (NC) fractionates with the inner membrane on sucrose density gradient centrifugation. Membranes of wild-type *S. Typhimurium* strain or a $\Delta prgHIJK$ isogenic mutant derivative, both expressing functional, FLAG-epitope tagged SpaR, were separated by sucrose density gradient centrifugation and fractionated into 11 fractions of equal volume. Proteins contained in the membrane fractions were separated by SDS/PAGE, and the levels of FLAG-epitope tagged SpaR, PrgH, PrgK, and InvG were analyzed by Western blotting. *Left* shows membrane fractions of wild-type *S. Typhimurium*. *Right* shows fractions of an isogenic mutant lacking the inner ring proteins PrgH and PrgK as well as the needle and inner rod proteins PrgI and PrgJ. The intensity of the bands corresponding to each protein was quantified using the Odyssey imaging system (Li-Cor), and values were standardized relative to the maximum intensity of each signal, which was assigned the arbitrary value of 10.

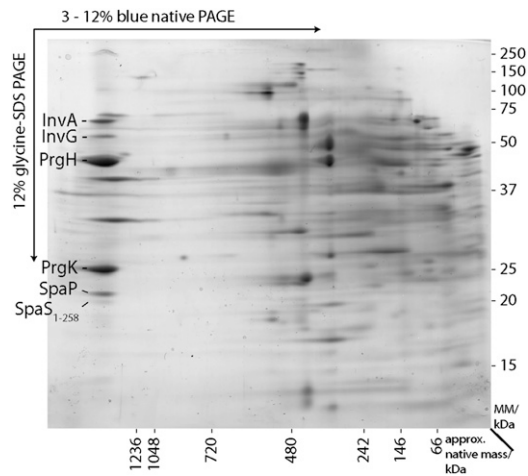


Fig. S2. Export apparatus components cofractionate with the NC. Protein complexes of DDM-solubilized inner membrane fractions of *S. Typhimurium* were separated by 2D BN-PAGE. Indicated proteins (*) were identified by LC-MS/MS or Western blotting.

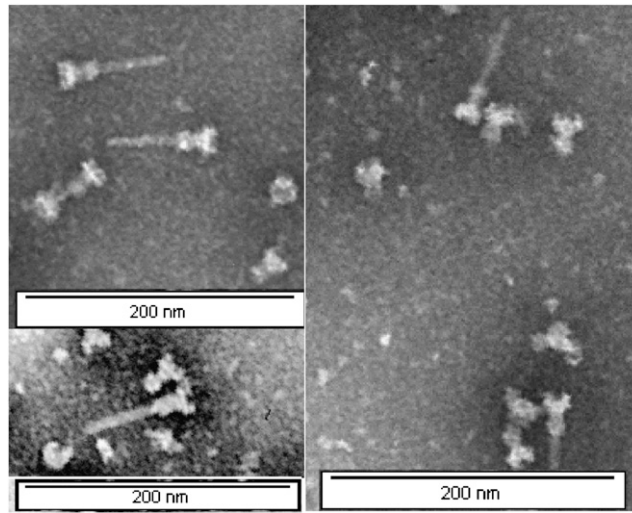


Fig. S3. Negative-stained electron microscopy images of NC samples obtained from *S. Typhimurium* harboring a $\text{SpaS}^{\text{N258A}}$ -FLAG allele. NCs were purified by immunoprecipitating $\text{SpaS}^{\text{N258A}}$ -FLAG from DDM-solubilized inner membrane fractions.

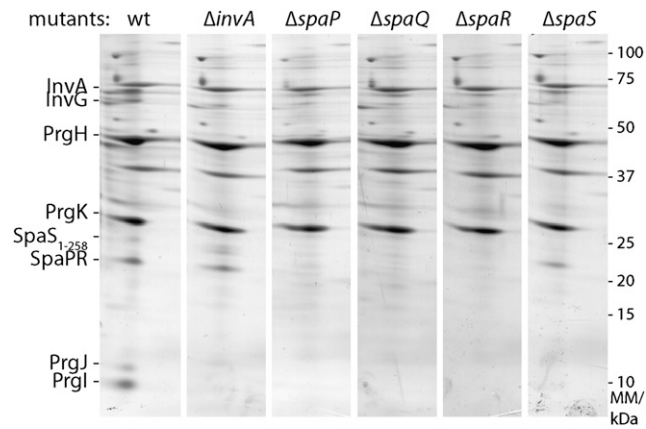


Fig. S4. Effect of mutations in export apparatus components on their recruitment to the NC. Protein complexes of DDM-solubilized inner membrane fractions of wild type and indicated mutants of *S. Typhimurium* were separated by 2D BN/Tricine SDS/PAGE, and gels were stained with colloidal Coomassie.

Table S2. Strains and plasmids

| Relevant genotypes of strains used in this study | | | |
|--|--|---------------|------------|
| Name | All strains are Flg ⁻ | Parent strain | Reference |
| SB762 | Wild type (SL1344, Flg ⁻) | SL1344 | (1) |
| SB905 | Wild type (SJW2941) | SJW2941 | (2) |
| SB1769 | SpaS ^{N258A} -FLAG | SL1344 | This study |
| SB1886 | SpaP-FLAG, <i>prgHIJK</i> | SL1344 | This study |
| SB1892 | P ^{ara} <i>hilA</i> , <i>spaPQRS</i> | SL1344 | This study |
| SB1901 | <i>invA</i> | SL1344 | This study |
| SB1902 | <i>spaP</i> | SL1344 | This study |
| SB1903 | <i>spaQ</i> | SL1344 | This study |
| SB1904 | <i>spaR</i> | SL1344 | This study |
| SB1905 | <i>spaS</i> | SL1344 | This study |
| SB1906 | InvA-FLAG | SL1344 | This study |
| SB1907 | SpaP-FLAG | SL1344 | This study |
| SB1909 | SpaR-FLAG | SL1344 | This study |
| SB1922 | <i>invA</i> , <i>spaPQRS</i> | SJW2941 | This study |
| SB1974 | SpaR-FLAG, <i>prgHIJK</i> | SL1344 | This study |
| SB1995 | InvA-FLAG, <i>spaP</i> | SL1344 | This study |
| SB1996 | InvA-FLAG, <i>spaQ</i> | SL1344 | This study |
| SB1997 | InvA-FLAG, <i>spaR</i> | SL1344 | This study |
| SB1998 | InvA-FLAG, <i>spaS</i> | SL1344 | This study |
| SB1999 | SpaP-FLAG, <i>invA</i> | SL1344 | This study |
| SB2000 | SpaP-FLAG, <i>spaQ</i> | SL1344 | This study |
| SB2001 | SpaP-FLAG, <i>spaR</i> | SL1344 | This study |
| SB2002 | SpaP-FLAG, <i>spaS</i> | SL1344 | This study |
| SB2007 | SpaR-FLAG, <i>invA</i> | SL1344 | This study |
| SB2008 | SpaR-FLAG, <i>spaP</i> | SL1344 | This study |
| SB2009 | SpaR-FLAG, <i>spaQ</i> | SL1344 | This study |
| SB2010 | SpaR-FLAG, <i>spaS</i> | SL1344 | This study |
| SB2011 | SpaS ^{N258A} -FLAG, <i>invA</i> | SL1344 | This study |
| SB2012 | SpaS ^{N258A} -FLAG, <i>spaP</i> | SL1344 | This study |
| SB2013 | SpaS ^{N258A} -FLAG, <i>spaQ</i> | SL1344 | This study |
| SB2014 | SpaS ^{N258A} -FLAG, <i>spaR</i> | SL1344 | This study |
| SB2018 | InvA-FLAG, <i>prgHIJK</i> | SL1344 | This study |
| SB2020 | SpaS ^{N258A} -FLAG, <i>prgHIJK</i> | SL1344 | This study |
| SB2091 | P ^{ara} <i>hilA</i> , <i>invA</i> | SL1344 | This study |
| SB2092 | P ^{ara} <i>hilA</i> , InvA-FLAG, <i>prgHIJK</i> | SL1344 | This study |
| SB2093 | P ^{ara} <i>hilA</i> , SpaP-FLAG, <i>prgHIJK</i> | SL1344 | This study |
| SB2100 | P ^{ara} <i>hilA</i> , InvA-FLAG | SL1344 | This study |
| SB2151 | P ^{ara} <i>hilA</i> , SpaP-FLAG | SL1344 | This study |
| SB2153 | P ^{ara} <i>hilA</i> , <i>invA</i> , <i>spaPQRS</i> | SL1344 | This study |
| SB2156 | P ^{ara} <i>hilA</i> , <i>spaPQRS</i> , <i>malEK::SpaP^{FLAG}QRS</i> | SL1344 | This study |
| SB2157 | P ^{ara} <i>hilA</i> , <i>invA</i> , <i>malEK::InvA-FLAG</i> | SL1344 | This study |
| SB2161 | <i>invA</i> | SJW2941 | This study |
| SB2162 | <i>spaP</i> | SJW2941 | This study |
| Plasmids used in this study | | | |
| Name | Genotype | | Reference |
| pSB667 | pBAD18- <i>hilA</i> | | (3) |
| pSB3398 | P ^{rhaBAD} , Kan ^R , SC101 ori | | This study |
| pSB3704 | pSB3398- <i>spaP^{FLAG}QRS</i> | | This study |
| pSB3405 | pSB3398- <i>invA^{FLAG}</i> | | This study |
| pSB3418 | pSB3398- <i>prgHIJKinvGH</i> | | This study |

1. Kaniga K, Tucker S, Trollinger D, Galán JE (1995) Homologs of the Shigella IpaB and IpaC invasins are required for Salmonella typhimurium entry into cultured epithelial cells. *J Bacteriol* 177:3965–3971.
2. Yamaguchi S, Fujita H, Ishihara A, Aizawa S, Macnab RM (1986) Subdivision of flagellar genes of Salmonella typhimurium into regions responsible for assembly, rotation, and switching. *J Bacteriol* 166:187–193.
3. Eichelberg K, Galán JE (1999) Differential regulation of Salmonella typhimurium type III secreted proteins by pathogenicity island 1 (SPI-1)-encoded transcriptional activators InvF and hilA. *Infect Immun* 67:4099–4105.